

Chromophobe renal cell carcinoma with sarcomatoid change: A case report

AE RI AHN^{1*}, SANG JAE NOH^{2*}, YOUNG BUM JEONG³ and KYOUNG MIN KIM¹

¹Department of Pathology, Research Institute of Clinical Medicine of Jeonbuk National University, Biomedical Research Institute of Jeonbuk National University Hospital, Research Institute for Endocrine Sciences, Jeonbuk National University Medical School, Jeonju, Jeollabuk-do 54907, Republic of Korea; ²Department of Forensic Medicine, Research Institute of Clinical Medicine of Jeonbuk National University, Biomedical Research Institute of Jeonbuk National University Hospital, Research Institute for Endocrine Sciences, Jeonbuk National University Medical School, Jeonju, Jeollabuk-do 54907, Republic of Korea; ³Department of Urology, Research Institute of Clinical Medicine of Jeonbuk National University, Biomedical Research Institute of Jeonbuk National University Hospital, Research Institute for Endocrine Sciences, Jeonbuk National University Medical School, Jeonju, Jeollabuk-do 54907, Republic of Korea

Received February 4, 2025; Accepted May 8, 2025

DOI: 10.3892/ol.2025.15117

Abstract. Chromophobe renal cell carcinoma (ChRCC) is a rare type of kidney cancer that is generally associated with a favorable prognosis. By contrast, RCC with sarcomatoid transformation exhibits a more aggressive clinical course, with its pathogenesis remaining largely unclear. The present study reports a case of ChRCC with sarcomatoid changes. A 54-year-old woman presented to the Department of Urology for evaluation of an incidentally detected left renal mass. Histological examination of the resected tumor revealed two distinct components: One with conventional ChRCC morphology and the other comprising highly pleomorphic, poorly differentiated cells. Next-generation sequencing of the two components revealed chromosomal losses in multiple chromosomes and variations in the *RNF46* gene. Based on these findings, a final diagnosis of ChRCC with sarcomatoid changes was made. Although the two components shared some

genetic changes, differences were also noted. The sarcomatoid area change carried chromosomal gain, single nucleotide variants and *MET* fusion compared with the conventional ChRCC component. Furthermore, while programmed cell death ligand 1 expression was negative in the conventional ChRCC component, >10% of the tumor cells in the sarcomatoid component were positive. Overall, the present case reveals novel genetic and immunohistochemical features of ChRCC with sarcomatoid changes.

Introduction

Chromophobe renal cell carcinoma (ChRCC) is a rare type of RCC, accounting for 5-7% of RCCs cases (1). ChRCC has a favorable prognosis compared with other RCC subtypes, including clear-cell RCC and papillary RCC (1). ChRCC originates from intercalated cells of the renal cortex, but sarcomatoid changes can occur in 2-8% of ChRCC cases. The presence of sarcomatoid changes in ChRCC significantly alters its clinical behavior, transforming it into a highly aggressive variant with a poor prognosis (2).

Sarcomatoid changes may occur in any RCC subtype, leading to the appearance of spindle-shaped pleomorphic cells that resemble sarcomas. These histological transformations are associated with rapid disease progression, increased metastatic potential and resistance to conventional therapies. While sarcomatoid changes are well documented in clear-cell and papillary RCC, their occurrence in ChRCC is rare and not fully understood (3).

The present study reports a case of ChRCC with sarcomatoid changes, highlighting distinct histopathological, genetic and immunohistochemical features. Through detailed next-generation sequencing (NGS) analysis, we aimed to identify the molecular changes responsible for this transformation. Analyzing the genetic alterations and immune profiles of sarcomatoid transformation in ChRCC may enhance therapeutic strategies and improve outcomes in affected patients.

Correspondence to: Professor Kyoung Min Kim, Department of Pathology, Research Institute of Clinical Medicine of Jeonbuk National University, Biomedical Research Institute of Jeonbuk National University Hospital, Research Institute for Endocrine Sciences, Jeonbuk National University Medical School, San 2-20 Keumam Dong, Dukjin, Jeonju, Jeollabuk-do 54907, Republic of Korea
E-mail: kmkim@jbnu.ac.kr

*Contributed equally

Abbreviations: ChRCC, chromophobe renal cell carcinoma; NGS, next-generation sequencing; CA, carbohydrate antigen; H&E, hematoxylin and eosin; KRT, keratin; FFPE, formalin-fixed paraffin-embedded; Indel, insertion-deletion; PD-L1, programmed cell death ligand 1; TKI, tyrosine kinase inhibitor

Key words: kidney, chromophobe renal cell carcinoma, sarcomatoid renal cell carcinoma, next-generation sequencing

Case report

A 54-year-old woman with no significant medical or family history presented to the Urology Department (Jeonbuk National University Hospital, Jeonju, South Korea) in February 2023 for evaluation of an incidentally detected left renal mass. Laboratory results were within normal ranges: Serum tumor markers, α -fetoprotein at 2.72 ng/ml (normal <7.0 ng/ml), carcinoembryonic antigen at 1.8 ng/ml (normal <5.2 ng/ml), carbohydrate antigen (CA) 19-9 at 9.0 U/ml (normal <34.0 U/ml) and CA125 at 28.4 U/ml (normal <35.0 U/ml). Computed tomography of the abdomen revealed a large left renal mass measuring 13x10 cm in maximum dimensions, with heterogeneous enhancement and irregular margins (Fig. 1A). The patient underwent an open radical nephrectomy for diagnosis and treatment.

Gross examination of the specimen revealed a tumor measuring 14.2x9.8 cm with two distinct components: A yellowish hard lesion (Fig. 1B; white arrow) and a white-grayish soft lesion (Fig. 1B; black arrow). The tumor exhibited an irregular margin and revealed a possible invasion into perinephric fat and adrenal tissue. For histopathological analysis, the resected specimen was fixed in 10% neutral buffered formalin at room temperature for 24 h. After fixation, the specimen was processed and embedded in paraffin. Each section was cut at 4 μ m thickness using a microtome and mounted on glass slides. Hematoxylin and eosin (H&E) staining was performed with hematoxylin staining for 3 min at room temperature, followed by eosin staining for 7 min at room temperature. All stained sections were observed under a light microscope. On histology, the yellowish hard lesion showed morphological features typical of ChRCC (Fig. 1C), while the white-grayish soft lesion showed large cells with marked nuclear pleomorphism and bizarre mitotic figures (Fig. 1D). The tumor cells had invaded the perinephric fat and adrenal glands (Fig. 1E). In a limited area, some foci showed a transition between lesion 1 and lesion 2 (Fig. 1F). The conventional and poorly differentiated ChRCC components exhibited contrasting immunohistochemical and special staining patterns. Staining was performed using an automated immunostainer (BenchMark ULTRA; Ventana Medical Systems, Inc.) according to the manufacturer's protocol. Tissue sections were fixed in 10% neutral buffered formalin at room temperature for 24 h, processed routinely and embedded in paraffin. Sections were cut at a thickness of 4 μ m and mounted on glass slides. All primary antibodies used were ready-to-use products provided by the manufacturer (Roche); therefore, no dilution was required. All staining steps, including deparaffinization, antigen retrieval, blocking, antibody incubation and detection, were carried out automatically under pre-optimized and standardized conditions according to the manufacturer's instructions. Hematoxylin was applied as a counterstain for 5 min at room temperature. All stained slides were examined using a light microscope. The conventional ChRCC component was positive for Keratin-7 (KRT-7; cat. no. 790-4462; Roche Tissue Diagnostics), KIT (CD117; cat. no. 790-7061; Roche Tissue Diagnostics) and pan-cytokeratin (cat. no. 760-2595; Roche Tissue Diagnostics) and negative for vimentin (cat. no. 760-2917; Roche Tissue Diagnostics), with positive staining for Hale's colloidal iron (cat. no. 860-009;

Roche Tissue Diagnostics). All immunohistochemical staining was performed using a Ventana BenchMark ULTRA immunostainer (Roche Tissue Diagnostics) according to the manufacturer's protocols. Chromogenic detection was performed using the OptiView DAB IHC Detection Kit (cat. no. 760-700; Roche Tissue Diagnostics), which contains biotinylated secondary antibody, streptavidin-HRP conjugate and DAB substrate. By contrast, the poorly differentiated components displayed the opposite staining pattern. However, focal KRT expression was observed in certain tumor cells within the poorly differentiated component (Fig. 2A-F). Targeted NGS-based genomic profiling was performed for the two components. Targeted NGS was performed using formalin-fixed, paraffin-embedded (FFPE) tumor tissues. H&E-stained slides were reviewed and the tumor area with sufficient viable tumor cells was marked for use as a guide for macrodissection. Tumor areas with >50% tumor cells were used for molecular examination. In brief, total nucleic acid was extracted from FFPE tissue using RecoverAll™ Total Nucleic Acid Isolation Kit (Ambion; Thermo Fisher Scientific, Inc.) according to the manufacturer's instructions. Library preparation for the OncoPrint® Comprehensive Assay Plus (Thermo Fisher Scientific, Inc.), which covers 2,737 amplicons (2,530 DNA + 207 RNA) within 143 cancer-related genes, was performed. An IonTorrent S5 XL platform was used for sequencing according to the manufacturer's specifications. The percentage of covered amplicons was 95%. Reads were aligned to the hg19 reference genome and variants with allele frequencies <3% were excluded. Both lesions shared an insertion-deletion (indel) variant, *RNF46* (c.349_350delCGinsA, p.Arg117ThrfsTer41). Copy number analysis identified identical chromosomal losses in lesions 1, 2, 6, 10, 13, 15, 17, 21 and X. Based on these findings, the pathological diagnosis confirmed ChRCC with sarcomatoid changes.

While the two components shared some genetic alterations, there were significant differences. The sarcomatoid component displayed distinct genetic features absent in the conventional ChRCC component. Copy number analysis identified chromosomal gains on chromosomes 1, 2, 6, 10, 13, 15, 17, 21 and X, contrasting with the chromosomal losses found in the ChRCC component (Fig. 3A and B). Additional genomic alterations included single nucleotide variants and indels in *TP53* (c.1176_1179delAGAC, p.Ter394IlefsTer27), *TSC2* (c.1675G>A, p.Asp559Asn), *NFI* (c.60+1G>A, p.?), *CDKN1B* (c.384_385insAG, p.His129SerfsTer17) and *MET-CAPZA2* fusion mutation. These data have been uploaded to Jeonbuk National University Hospital repository.

To assess the immunotherapeutic potential, immunohistochemical staining for programmed cell death ligand 1 (PD-L1; cat. no. 790-4905; Roche Tissue Diagnostics) was performed. Chromogenic detection was performed using the OptiView DAB IHC Detection Kit (cat. no. 760-700; Roche Tissue Diagnostics), which contains biotinylated secondary antibody, streptavidin-HRP conjugate and DAB substrate. Immunohistochemical staining for PD-L1 was performed using an automated immunostainer (BenchMark ULTRA; Ventana Medical Systems, Inc.) according to the manufacturer's protocol. Tissue sections were fixed in 10% neutral buffered formalin at room temperature for 24 h, processed routinely and embedded in paraffin. Sections were cut at a thickness

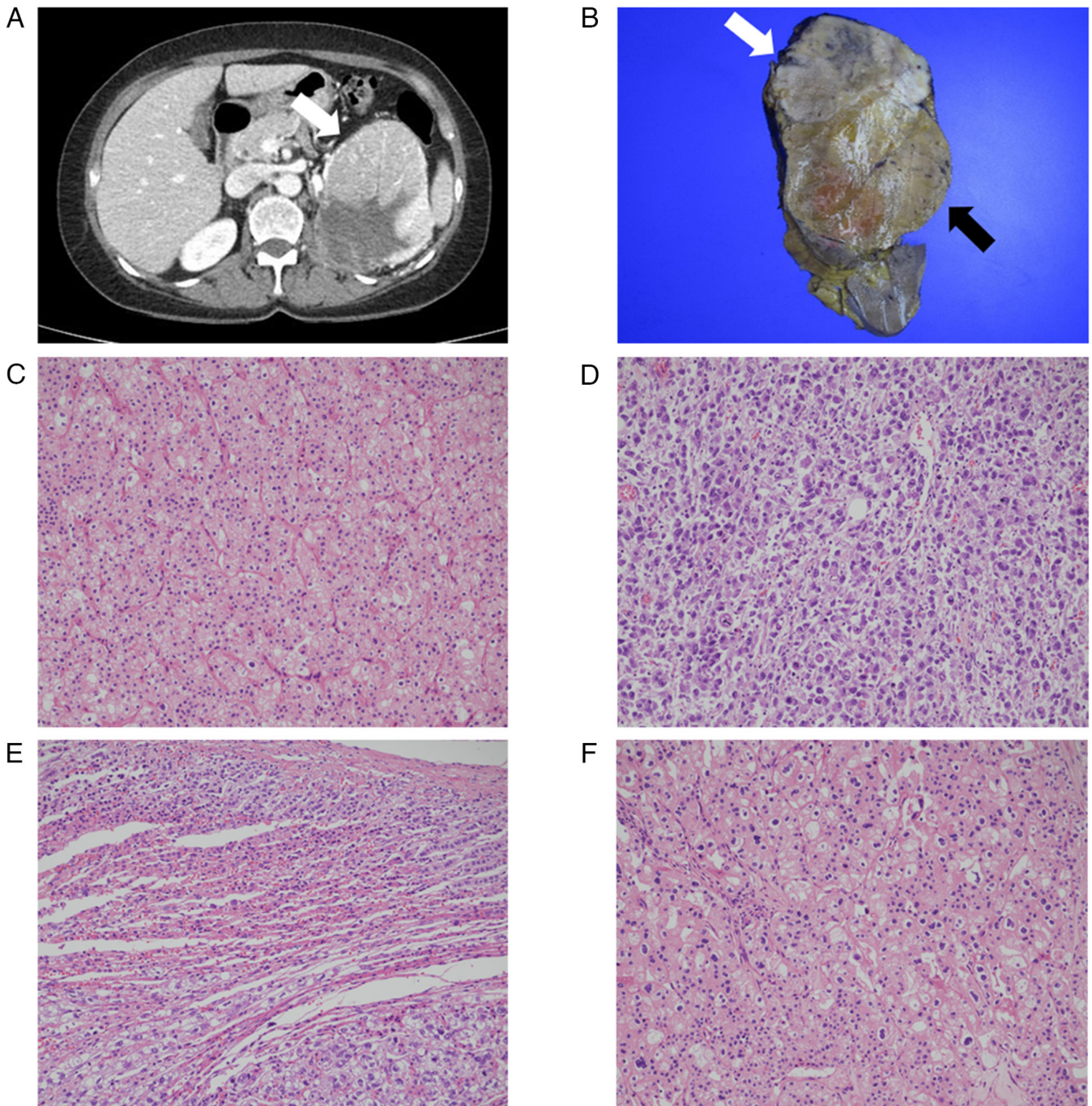


Figure 1. Radiological and histopathological findings of chromophobe renal cell carcinoma with sarcomatoid change. (A) Computed tomography demonstrated a 13 cm-sized mass in the upper pole of left kidney (white arrow). (B) The resected specimen revealed irregular margined tumor measuring 14.2x9.8 cm. The tumor consisted of following two components: Yellowish hard lesion (black arrow, lesion 1) and white-grayish soft lesion (white arrow, lesion 2). (C) Chromophobe renal cell carcinoma consisted of the tumor cells are arranged in solid sheets, separated by hyalinized vascular septa. Hyperchromatic nuclei and the presence of perinuclear haloes are characteristic (H&E; magnification, x200). (D) Sarcomatoid component showed large-sized cells with marker nuclear pleomorphism and bizarre mitotic figures (H&E; magnification, x200). (E) Sarcomatoid component invaded the adrenal gland (H&E; magnification, x200). (F) The transition between chromophobe renal cell carcinoma component and sarcomatoid component was identified (H&E; magnification, x200). H&E, hematoxylin and eosin.

of 4 μ m and mounted on glass slides. All primary antibodies used were ready-to-use products provided by the manufacturer (Roche); therefore, no dilution was required. All staining steps, including deparaffinization, antigen retrieval, blocking, antibody incubation and detection, were carried out automatically under pre-optimized and standardized conditions according to the manufacturer's instructions. Hematoxylin was applied

as a counterstain for 5 min at room temperature. All stained slides were examined using a light microscope. The ChrCC component was negative for PD-L1, whereas the area showed $\geq 10\%$ positivity (Fig. 2G and H).

Following diagnosis, the patient underwent chemotherapy with nivolumab and cabozantinib. The patient received chemotherapy with cabozantinib 40 mg (orally) and nivolumab

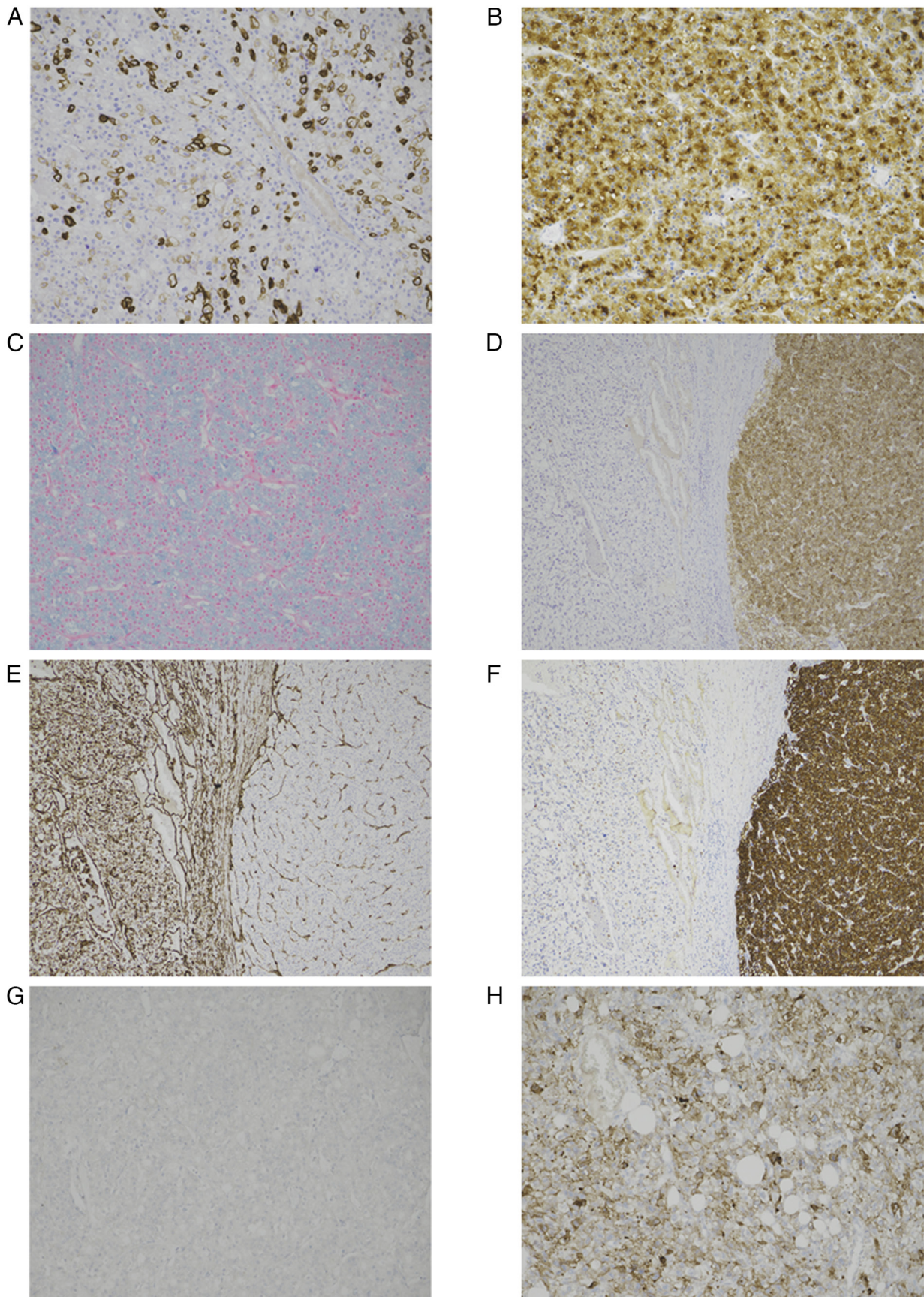


Figure 2. Immunohistochemical findings of chromophobe renal cell carcinoma with sarcomatoid change. Chromophobe renal cell carcinoma showed strong positivity for (A) KRT7 and (B) Hale's colloidal iron stain (magnification, x200). Chromophobe renal cell carcinoma and sarcomatoid component showed opposing staining for (C) KIT (CD117) and (D) vimentin (magnification, x100). KRT showed (E) diffuse strong positivity in the chromophobe renal cell carcinoma component (magnification, x100) and (F) focal positivity in the sarcomatoid component (magnification, x200). Staining for programmed cell death ligand 1 revealed that expression was (G) negative in the chromophobe renal cell carcinoma component and (H) positive in the sarcomatoid component (magnification, x200). KRT, keratin.

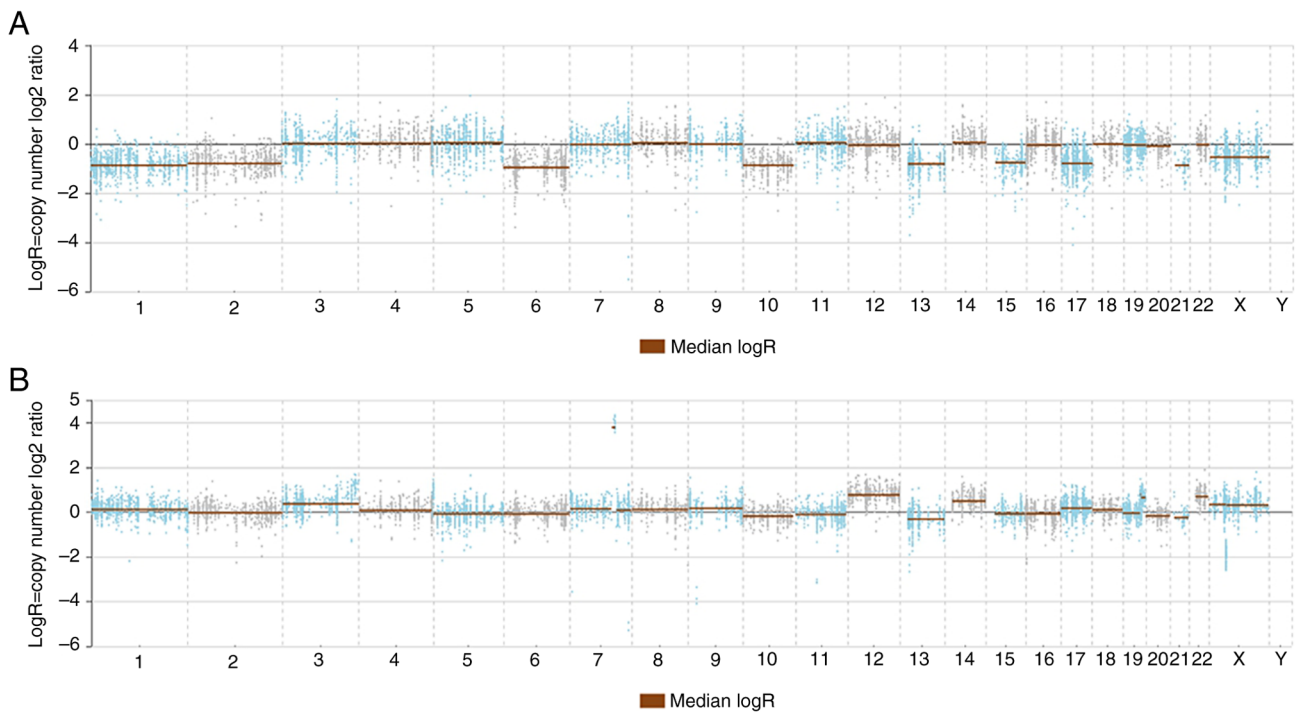


Figure 3. Next-generation sequencing of chromophobe renal cell carcinoma with sarcomatoid differentiation. (A) In the chromophobe renal cell carcinoma component, copy number analysis identified chromosomal loss in chromosomes 1, 2, 6, 10, 13, 15, 17, 21 and X. (B) The sarcomatoid differentiation component exhibited distinct genetic features not seen in the chromophobe renal cell carcinoma component. Copy number analysis identified chromosomal gains in chromosomes 1, 2, 6, 10, 13, 15, 17, 21 and X.

240 mg (orally). After treatment for 2 consecutive days, the patient exhibited symptoms of colitis and immune-mediated pneumonitis. Despite adjuvant chemotherapy, the tumor progressed and metastasized to multiple organs, including the lungs, liver, bones and lymph nodes. The patient's condition rapidly deteriorated due to hypercalcemia caused by multiple metastasis, and the patient died in April 2023.

Discussion

ChRCC was first identified as a distinctive subtype of RCC by Thoenes in 1985 (4). ChRCC is uncommon subtype with generally favorable prognosis compared to clear-cell RCC or papillary RCC, exhibiting a 5-year survival rate of 78-100% and a 10-year survival rate of 80-90% (5). However, sarcomatoid differentiation significantly alters its clinical course transforming ChRCC into an aggressive variant with poor outcomes (2). Although documented across all RCC subtypes, sarcomatoid transformation remains poorly understood in ChRCC because of its rarity. The present case highlights the histopathological, genetic and immunohistochemical differences between conventional ChRCC and its sarcomatoid counterparts and provides insights into the molecular changes that drive sarcomatoid transformation.

In the present case, the coexistence of two distinct tumor components, one conventional ChRCC and the other sarcomatoid, along with the presence of a transitional area, suggested that sarcomatoid transformation arose from pre-existing ChRCC cells by acquiring additional molecular alterations that drive aggressive behavior. NGS analysis revealed that both components shared certain genetic changes such as the *RNF46* variant and chromosomal loss, whereas the sarcomatoid

component exhibited additional distinct genetic alterations. The conventional ChRCC component exhibited loss of chromosomes 1, 2, 6, 10, 13, 15, 17, 21 and X. Among these, the loss of chromosomes 1, 2, 6, 10 and 17 are recognized as hallmarks of ChRCC (6,7). The NGS analysis revealed that additional alterations in the sarcomatoid component were chromosomal gains detected in chromosomes 3, 5, 7, 9, 12, 13, 14, 19, 22 and X. These chromosomal gains have also been reported in previous literature on sarcomatoid ChRCC, suggesting that they may contribute to the sarcomatoid transformation of ChRCC (7). Additionally, in the sarcomatoid component, mutations in key tumor suppressor genes such as *TP53*, *TSC2* and *NF1* were observed, along with the detection of a *MET-CAPZA2* fusion. These mutations could open possibilities for the sarcomatoid differentiation of ChRCC component.

The *MET* gene, encoding a tyrosine kinase receptor in the hepatocyte growth factor/scatter factor pathway, is implicated in various oncogenic processes, including cell proliferation, angiogenesis, invasion and metastasis (8,9). Among *MET* alteration, *MET* fusions have been identified as oncogenic drivers in various cancers, such as lung cancer, glioma, colorectal cancer and cholangiocarcinoma (10). In RCC, *MET* alterations, particularly *MET* exon 14 skipping mutations and *MET* amplifications, have been associated with sarcomatoid transformation and poor prognosis (11). However, to the best of our knowledge, no studies have reported *MET* fusion in the sarcomatoid transformation of ChRCC at present. The present study's identification of the *MET-CAPZA2* fusion in the sarcomatoid component suggests that aberrant *MET* activation may play a key role in driving the aggressive phenotype observed in this case.

In addition, in the present case, the *TP53* mutation was exclusively detected in the sarcomatoid component. *TP53* is a well-known tumor suppressor gene that regulates cell cycle arrest, DNA repair and apoptosis. Loss-of-function *TP53* mutations are commonly associated with high-grade, undifferentiated and aggressive tumors, as they lead to increased genomic instability, uncontrolled cell proliferation and resistance to apoptosis (12). In RCC, *TP53* mutations are frequently observed in sarcomatoid dedifferentiation and are associated with poor prognosis and resistance to immune checkpoint inhibitors (13,14).

The sarcomatoid component in the present case harbored additional alterations in *TSC2* and *NF1*, both of which are tumor suppressor genes involved in the mTOR and RAS signaling pathways, respectively (15,16). *TSC2* mutations can lead to constitutive mTOR activation, driving cellular proliferation and metabolic reprogramming, which contribute to an aggressive tumor phenotype (15). Meanwhile, *NF1* mutations disrupt the negative regulation of the RAS-MAPK pathway, promoting tumor growth and invasion. Loss of *NF1* has also been associated with resistance to targeted therapies, further highlighting the treatment challenges in sarcomatoid RCC (16).

Studies have demonstrated that targeting *MET* fusions with selective *MET* tyrosine kinase inhibitors (TKI) such as savolitinib and crizotinib can be effective in various cancers, including non-small cell lung cancer and other solid tumors (17). For example, patients with *MET* fusion-positive tumors, including lung and hepatobiliary cancers, respond to crizotinib in clinical trials (10,18). These findings support the potential of *MET* TKIs in the treatment of *MET* fusion-driven cancers and reinforce their role in precision medicine. Management of ChRCC with sarcomatoid changes based on genetic alterations has not yet been standardized. Although *MET* fusion was identified in the present case, we were unable to use TKIs for treatment. However, we hypothesize that targeted therapies against *MET* should be considered as future treatment strategies for sarcomatoid ChRCC, although such approaches need to be fully explored in clinical trials. The heterogeneity of *MET* alterations influences sensitivity to *MET* TKI and also serve as a predictive biomarker for improving patient selection. A previous study highlighted the pivotal role of the *MET* pathway in RCC and provide a comprehensive review of clinical data on multiple drugs targeting the *MET* pathway. Combination strategies of *MET* TKI and immune checkpoint inhibitors could lead to sustained and deep responses in RCC (19).

Another important finding in the present case was the differential expression of PD-L1 between conventional ChRCC and the sarcomatoid components. PD-L1 positivity in >10% of sarcomatoid tumor cells suggests that immune checkpoint inhibitors such as nivolumab may be potential therapeutic options (20). Aberrant PD-L1 expression is associated with high-grade histology such as sarcomatoid differentiation. A previous study has shown that sarcomatoid components exhibit higher PD-L1 expression than non-sarcomatoid components (21). The present case is similar to those of previous studies (20,21). In the present case, the ChRCC component was negative for PD-L1, whereas the sarcomatoid

component showed $\geq 10\%$ positivity. Aberrant PD-L1 expression in the sarcomatoid component could indicate the biological distinctiveness of sarcomatoid differentiation and could have potential therapeutic implications. Because previous studies suggest that higher PD-L1 expression is associated with a higher histological grade in RCC, it is important to compare the immune checkpoint marker such as PD-L1 between the classical RCC component and the sarcomatoid component specifically (22). However, in the present study, despite the use of nivolumab, the patient's tumor continued to progress, leading to multiple organ metastases and death within 1 month. This rapid progression highlights the aggressive nature of sarcomatoid ChRCC and suggests that while immune checkpoint inhibitors may offer some benefits, they may not be sufficient as a monotherapy, particularly in advanced or metastatic cases.

The current patient's poor response to combination therapy with nivolumab and cabozantinib underscores the need for further research on more effective treatment strategies for sarcomatoid ChRCC. A previous review article reported that combination therapy using cabozantinib and nivolumab can make treatment more complex by causing an immunosuppressive state and drug toxicity (23). This could be possible explanation for the present patient's poor response to combination therapy. Due to the molecular heterogeneity observed between the conventional and sarcomatoid components, a more personalized therapeutic approach targeting specific genetic alterations and immune profiles may be necessary to improve outcomes in patients with this aggressive variant of RCC. For instance, the combination of immune checkpoint inhibitors with targeted therapies against *MET*, *TP53* and other genetic alterations identified in sarcomatoid ChRCC should be explored in future studies.

In conclusion, the present case highlights the unique molecular and immunohistochemical characteristics of ChRCC with sarcomatoid transformation. The distinct genetic differences between the two components emphasize the complex molecular landscape of this tumor and highlight the challenges in treating sarcomatoid ChRCC. Further research is needed to better understand the mechanisms driving sarcomatoid transformation and to develop more effective and tailored therapeutic strategies for patients with this rare and aggressive form of RCC.

Acknowledgements

Not applicable.

Funding

This paper was supported by the Fund of Biomedical Research Institute, Jeonbuk National University Hospital.

Availability of data and materials

The NGS data generated in the present study may be found in the Ion Reporter under the following URL: https://figshare.com/articles/dataset/4_S23_3641_A4_2_study_v1_b1dcd489-a2c3-4355-b6c7-42e61ad47e55_2023-04-04_21-51-44-090_All_zip/29002592?file=54388502. The other data generated

in the present study may be requested from the corresponding author.

Authors' contributions

ARA and KMK conceptualized the study and wrote the original manuscript. ARA and SJN searched the literature and obtained case-related data. KMK and YBJ analyzed data and relevant literature. KMK reviewed and edited the final draft. KMK and SJN confirm the authenticity of all the raw data. All authors read and approved the final version of the manuscript.

Ethics approval and consent to participate

This case report was approved by Jeonbuk National University Hospital Institutional Review Board (approval no. IRB 2023-07-004). This case report was conducted in accordance with the Declaration of Helsinki of 1975.

Patient consent for publication

Patient consent was obtained for publication of images and data.

Competing interests

The authors declare that they have no competing interests.

References

- Moch H, Amin MB, Berney DM, Comp erat EM, Gill AJ, Hartmann A, Menon S, Raspollini MR, Rubin MA, Srigley JR, *et al*: The 2022 World Health Organization classification of tumours of the urinary system and male genital organs-part A: Renal, penile, and testicular tumours. *Eur Urol* 82: 458-468, 2022.
- Lobo J, Ohashi R, Amin M-B, Berney DM, Comp erat EM, Cree IA, Gill AJ, Hartmann A, Menon S, Netto GJ, *et al*: WHO 2022 landscape of papillary and chromophobe renal cell carcinoma. *Histopathology* 81: 426-438, 2022.
- Shuch B, Bratslavsky G, Linehan WM and Srinivasan R: Sarcomatoid renal cell carcinoma: A comprehensive review of the biology and current treatment strategies. *Oncologist* 17: 46-54, 2012.
- Thoenes W, St orkel S and Rumpelt HJ: Human chromophobe cell renal carcinoma. *Virchows Arch B Cell Pathol Incl Mol Pathol* 48: 207-217, 1985.
- Bian L, Duan J, Wang X, Yang Y, Zhang X and Xiao S: Sarcomatoid chromophobe renal cell carcinoma: A case report and review of the literature. *Am J Case Rep* 20: 1225-1230, 2019.
- Brunelli M, Gobbo S, Cossu-Rocca P, Cheng L, Hes O, Delahunt B, Pea M, Bonetti F, Mina MM, Ficarra V, *et al*: Chromosomal gains in the sarcomatoid transformation of chromophobe renal cell carcinoma. *Mod Pathol* 20: 303-309, 2007.
- Brunelli M, Eble JN, Zhang S, Martignoni G, Delahunt B and Cheng L: Eosinophilic and classic chromophobe renal cell carcinomas have similar frequent losses of multiple chromosomes from among chromosomes 1, 2, 6, 10, and 17, and this pattern of genetic abnormality is not present in renal oncocytoma, and this pattern of genetic abnormality is not present in renal oncocytoma. *Mod Pathol* 18: 161-169, 2005.
- Guo R, Luo J, Chang J, Rekhtman N, Arcila M and Drilon A: MET-dependent solid tumours-molecular diagnosis and targeted therapy. *Nat Rev Clin Oncol* 17: 569-587, 2020.
- Rhoades Smith KE and Bilen MA: A review of papillary renal cell carcinoma and MET inhibitors. *Kidney Cancer* 3: 151-161, 2019.
- Turpin A, Descarpentries C, Gr egoire V, Farchi O, Cortot AB and Jamme P: Response to capmatinib in a MET fusion-positive cholangiocarcinoma. *Oncologist* 28: 80-83, 2023.
- Liu XW, Chen XR, Rong YM, Lyu N, Xu CW, Wang F, Sun WY, Fang SG, Yuan JP, Wang HJ, *et al*: MET exon 14 skipping mutation, amplification and overexpression in pulmonary sarcomatoid carcinoma: A multi-center study. *Transl Oncol* 13: 100868, 2020.
- Amendolare A, Marzano F, Petruzzella V, Vacca RA, Guerrini L, Pesole G, Sbis  E and Tullio A: The underestimated role of the p53 pathway in renal cancer. *Cancers (Basel)* 14: 5733, 2022.
- Bi M, Zhao S, Said JW, Merino MJ, Adeniran AJ, Xie Z, Nawaf CB, Choi J, Belldegrun AS, Pantuck AJ, *et al*: Genomic characterization of sarcomatoid transformation in clear cell renal cell carcinoma. *Proc Natl Acad Sci USA* 113: 2170-2175, 2016.
- Carlsen L, Zhang S, Tian X, De La Cruz A, George A, Arnoff TE and El-Deiry WS: The role of p53 in anti-tumor immunity and response to immunotherapy. *Front Mol Biosci* 1: 1148389, 2023.
- Kwiatkowski DJ, Choueiri TK, Fay AP, Rini BI, Thorner AR, de Velasco G, Tyburczy ME, Hamieh L, Albiges L, Agarwal N, *et al*: Mutations in TSC1, TSC2, and MTOR are associated with response to rapalogs in patients with metastatic renal cell carcinoma. *Clin Cancer Res* 22: 2445-2452, 2016.
- Giraud JS, Bi che I, Pasmant   and Tlemsani C: NF1 alterations in cancers: Therapeutic implications in precision medicine. *Expert Opin Investig Drugs* 32: 941-957, 2023.
- Recondo G, Che J, J anne PA and Awad MM: Targeting MET dysregulation in cancer. *Cancer Discov* 10: 922-934, 2020.
- Cheng W, Xu T, Yang L, Yan N, Yang J and Fang S: Dramatic response to crizotinib through MET phosphorylation inhibition in rare TFG-MET fusion advanced squamous cell lung cancer. *Oncologist* 30: oyael66, 2025.
- Nandagopal L, Sonpavde GP and Agarwal N: Investigational MET inhibitors to treat renal cell carcinoma. *Expert Opin Investig Drugs* 28: 851-860, 2019.
- Goodman AM, Piccioni D, Kato S, Boichard A, Wang HY, Frampton G, Lippman SM, Connelly C, Fabrizio D, Miller V, *et al*: Prevalence of PDL1 amplification and preliminary response to immune checkpoint blockade in solid tumors. *JAMA Oncol* 4: 1237-1244, 2018.
- Thompson RH, Kuntz SM, Leibovich BC, Dong H, Lohse CM, Webster WS, Sengupta S, Frank I, Parker AS, Zincke H, *et al*: Tumor B7-H1 is associated with poor prognosis in renal cell carcinoma patients with long-term follow-up. *Cancer Res* 66: 3381-3385, 2006.
- Kawakami F, Sircar K, Rodriguez-Canales J, Fellman BM, Urbauer DL, Tamboli P, Tannir NM, Jonasch E, Wistuba II, Wood CG and Karam JA: Programmed cell death ligand 1 and tumor-infiltrating lymphocyte status in patients with renal cell carcinoma and sarcomatoid dedifferentiation. *Cancer* 123: 4823-4831, 2017.
- McGregor B, Mortazavi A, Cordes L, Salabao C, Vandlik S and Apolo AB: Management of adverse events associated with cabozantinib plus nivolumab in renal cell carcinoma: A review. *Cancer Treat Rev* 103: 102333, 2022.



Copyright   2025 Ahn et al. This work is licensed under a Creative Commons Attribution-NonCommercial-NoDerivatives 4.0 International (CC BY-NC-ND 4.0) License.